이학석사 학위논문

항암 면역치료를 위한 PBK 타겟 항암 백신 개발에 관한 연구

Development of cancer vaccine targeting PBK for cancer immunotherapy

울 산 대 학 교 대 학 원

의 과 학 과

김 혜 빈

Development of cancer vaccine targeting PBK for cancer immunotherapy

지 도 교 수　　진 형 승

이 논문을 이학석사학위 논문으로 제출함

2024년　8월

울 산 대 학 교 대 학 원

의 과 학 과

김 혜 빈

김혜빈의 이학석사학위 논문을 인준함

심사위원 노진경

심사위원 오수진

심사위원 진형승

울 산 대 학 교 대 학 원

2024년 8월

ABSTRACTS

Development of cancer vaccine targeting PBK for cancer immunotherapy

Although immune checkpoint inhibitors (ICI) have shown efficacy in some colon cancer patients with deficient DNA mismatch repair or high microsatellite instability, there remains a significant need for developing effective treatments for colon cancer. PBK, a serine/threonine kinase, regulates cell cycle and mitotic progression. Through bioinformatic analysis, high PBK expression was found to correlate with better prognosis in colon cancer. Immune profiling revealed that PBK-high colon cancers exhibit increased infiltration of cytotoxic immune cells and reduced infiltration of immunosuppressive cells, suggesting a favorable tumor microenvironment. These findings highlight PBK's potential as an immunotherapeutic target in colon cancer treatment. his study also explores the potential of PBK peptides for targeted immunotherapy in cancer treatment. Predictive algorithms and binding affinity analyses identified specific peptides with high affinity for HLA-A*02:01 molecules, demonstrated through increased cell surface stabilization and prolonged dissociation times. These peptides induced significant peptide-specific cytotoxic T cell responses, evidenced by their ability to specifically lyse target cells, underscoring their potential for targeted cancer immunotherapy. mouse model was established to evaluate PBK-targeted therapies, confirming high PBK expression in cancer cell lines but not in normal tissues. Deletion of the PBK gene in CT26 cells revealed that its deficiency did not affect cell proliferation or immune checkpoint molecule expression. However, PBK-deficient tumors in syngeneic mouse models exhibited reduced growth and increased infiltration of CD4+ and CD8+ T cells, with elevated granzyme B expression in CD8+ T cells, indicating enhanced cytotoxic potential. This study underscores the therapeutic potential of targeting PBK to augment antitumor immune responses, paving the way for novel immunotherapeutic strategies in cancer treatment.

CONTENTS

LIST OF FIGURES

ABBREVIATIONS

MAPK: mitogen-activated protein kinase

PD-1: Programmed cell death receptor-1

PD-L1: Programmed cell death receptor-Ligand1

TIM-3: T cell immunoglobulin-3

dMMR : deficient DNA mismatch repair

MSI : microsatellite instability

MSS : microsatellite stable

pHLA : peptide-human leukocyte antigen

MHC: major histocompatibility complex

TME: Tumor microenvironment

TIL: Tumor-infiltrating lymphocyte

TAAs : Tumor-associated antigens

TSAs : Tumor-specific antigens

TCGA : The Cancer Genome Atlas

TAP : Transporter associated with antigen processing

MFI: median fluorescence intensity

GM-CSF: granulocyte-macrophage colony-stimulating factor

DCs : dendritic cells

CTLs: cytotoxic T lymphocytes

OS: overall survival

DFS: disease-free survival

HR: hazard ratio

ICI: immune checkpoint inhibitor

PBMC: Peripheral blood mononuclear cell

FACS : fluorescence-activated cell sorter

CRC : Colorectal cancer

COAD: colon adenocarcinoma

HNSC: head and neck squamous carcinoma

HPV: human papillomavirus

ACC: adenoid cystic carcinoma

LUAD: lung adenocarcinoma

LGG: low-grade gliomas

KIRP: Kidney renal papillary cell carcinoma

MESO: malignant mesothelioma

PADD: pancreatic adenocarcinoma

SARC: sarcoma

KIRC: kidney renal clear cell carcinoma

THYM: Thymoma

Treg: regulatory T

CTA: Cancer/testis antigens

ANNs: artificial neural networks

KO: knockout

TPM: transcripts per million

BLCA: bladder urothelial carcinoma

BRCA: breast invasive carcinoma

CESC: cervical squamous cell carcinoma

CHOL: cholangiocarcinoma

DLBC: diffuse large B-cell lymphoma

ESCA: esophageal carcinoma

GBM: glioblastoma multiforme

KICH: kidney chromophobe

LAML: acute myeloid leukemia

LIHC: liver hepatocellular carcinoma

LUSC: lung squamous cell carcinoma

OV: ovarian serous cystadenocarcinoma

PAAD: pancreatic adenocarcinoma

PCPG: pheochromocytoma and paraganglioma

PRAD: prostate adenocarcinoma

READ: rectum adenocarcinoma

SKCM: skin cutaneous melanoma

STAD: stomach adenocarcinoma

TGCT: testicular germ cell tumors

THCA: thyroid carcinoma

UCEC: uterine corpus endometrial carcinoma

UCS: uterine carcinosarcoma

UVM: uveal melanoma

GrzB: granzyme B

CRISPR: clustered regularly interspaced short palindromic repeats

1. Introduction

1.1. PBK

T-lymphokine-activated killer-cell-originated protein kinase (TOPK), also known as PDZ-binding kinase (PBK), is a novel mitotic serine/threonine protein kinase[1, 2].

This kinase is found in abundance in rapidly dividing tissues such as the placenta, testis, T-LAK cells, activated lymphoid cells, and lymphoid tumors, but its presence is minimal to none in non-dividing normal tissues like the adult brain[3, 4].

PBK is expressed both in the cytoplasm and the nucleus. In tumor cells or during mitosis, it may be expressed exclusively in the nucleus. It is particularly around chromosomal surfaces during prophase and metaphase. Moreover, both PBK protein expression and its activation are regulated by the cell cycle[5, 6].

PBK is part of the MEK3/6-related MAPKK family. It has characteristic serine/threonine kinase subdomains. It also has a PDZ-binding motif at its C-terminus. This motif allows it to specifically bind to the PDZ proteins. When activated, PBK can phosphorylate p38 MAPK and histone H3. Its kinase activity is regulated by the cell cycle. It activates only during mitosis after phosphorylation by the CDK1/cyclin B1 complex. This activation involves PBK's interaction with the CDK1/cyclin B1 complex at the mitotic spindle. This interaction triggers its phosphorylation. This, in turn, enhances its ability to bind to the CDK1/cyclin B1 complex. It achieves this by phosphorylating and inactivating PP1α. These findings suggest that PBK plays a role in regulating cell proliferation and the cell cycle[2, 7, 8].

Overexpression of PBK in oncogenic pathways has been linked to tumor proliferation, metastasis, and anti-apoptosis. This overexpression allows tumor cells to circumvent the natural surveillance mechanism at the G2/M checkpoint. It leads to abnormal entry into the mitotic phase by phosphorylating histone H3 at Ser10. Additionally, it involves downregulating the tumor suppressor p53 and upregulating the cyclin-dependent kinase inhibitor p21, thereby contributing to tumorigenesis[9, 10]. On the other hand, suppressing PBK diminishes its tumorigenic properties. This is achieved by reducing the phosphorylation and activation of mitogen-activated protein (MAP) kinase, including ERK2 and P38. It also involves inhibiting the expression of mutant p53 and Akt activation[11-15]. In turn, phosphorylated ERK2 can phosphorylate PBK and increase its kinase activity. This creates a positive feedback loop between PBK and ERK2. PBK can also activate the interaction between the

transcriptional factor β-catenin and its transcriptional coactivators TCF/LEF. This interaction upregulates the transcription of matrix metalloproteinases MMP-2 and MMP-9, thereby enhancing the invasiveness and metastasis of tumor cells[5].

These studies collectively indicate that PBK could act as both a diagnostic/prognostic marker and a therapeutic target in tumors.

1.2. Colon cancer and immunotherapy

Colorectal cancer (CRC) is the second leading cause of cancer-related deaths worldwide. Over recent decades, the introduction of more systematic and effective screening methods has enabled early detection. Moreover, advancements in treatment have significantly reduced both the incidence and death rates from CRC. Treatments targeting CRC include chemotherapy, surgery, radiotherapy, and strategies for addressing metastatic disease[16].

The advent of immunotherapy has transformed the field of oncology, including CRC, by harnessing the power of the immune system to fight certain cancers. The immune system includes regulatory pathways that are influenced by co-stimulatory and co-inhibitory signals. Immune checkpoints act as negative regulators, restricting the T-cell-mediated immune responses against cancer cells. However, cancer cells can evade this anti-tumor response. They achieve this by exploiting these immune checkpoints, upregulating specific molecules that interact with inhibitory receptors on immune cells[17, 18]. To combat this immune evasion, immune checkpoint inhibitors (ICIs) have been developed. These inhibitors target the inhibitory receptors such as PD-1, PD-L1, and CTLA-4. ICIs have proven effective in overcoming immune surveillance evasion by blocking these inhibitory signals. After their initial approval for melanoma treatment, ICIs have been approved for various cancers[19].

Studies have identified a subset of CRC with a distinct molecular profile characterized by microsatellite instability (MSI) due to deficient DNA mismatch repair (dMMR), which is more responsive to immunotherapy. This subset of tumors, with a high tumor mutational burden, produces unique neoantigens that attract T-cells, making them more vulnerable to immunotherapy[20, 21].

Only 15% of CRCs are classified as MSI-High (MSI-H), which are more commonly found in right-sided tumors. The remaining 85% are microsatellite stable (MSS) with proficient mismatch repair (pMMR). In metastatic CRC (mCRC), only about 5% of tumors are MSI-H. This disparity may reflect better immune surveillance due to microsatellite instability, preventing advanced cancer progression, or indicate a change in microsatellite status during cancer progression[22].

ICIs have shown remarkable efficacy across all stages of MSI-H/dMMR CRC[23, 24]. While there

are no approved ICIs for MSS/pMMR CRC patients yet, ongoing trials exploring combinations of ICIs with targeted therapy, radiotherapy, and chemotherapy are eagerly awaited.

1.3. Cancer vaccine

Infection by a wide variety of foreign pathogens can now be controlled through the use of vaccines. However, cancer, which arises from random mutational events as a disease of altered self, has been much less amenable to this approach. There have been significant efforts to generate vaccines against solid and hematologic malignancies. These efforts use a variety of platforms[25].

T cells are a crucial component of the adaptive immune system. They help to facilitate antitumor rejection and prevent disease recurrence. To accomplish this, tumor antigens are processed by antigen-presenting cells. These cells present the antigens to T cells as a peptide-human leukocyte antigen (pHLA) complex[26, 27].

Tumor antigens can be classified as either tumor-associated antigens (TAAs) or tumor-specific antigens (TSAs). TAAs are autoantigens expressed in normal tissues but are overexpressed in cancers. TSAs are produced exclusively by tumor cells and are most often generated through nonsynonymous somatic mutations. Although each antigen class has unique advantages for vaccine development, they also have limitations that hinder their clinical success[28]. For TAAs, challenges include peripheral and central immune tolerance. This tolerance leads to the failure of removal of cells that express self-antigens. There is also a risk of autoimmunity against corresponding normal tissues and tumor heterogeneity[29]. TSAs have the advantage of being tumor-specific. This lowers the risk of autoimmunity and allows bypassing of thymic-negative selection[30, 31]. However, identifying TSA neoantigens for vaccine development is challenging because only about 1% of mutations produce neoantigens that trigger spontaneous tumor infiltrating lymphocytes (TIL) responses[32]. In both TAAs and TSAs, cancer immunoediting can lead to antigen loss, enhancing antitumor immunity evasion[33].

In general, the most common cancer vaccine platforms are peptide-based, cell-based, RNA, DNA, and viral. Although all have their strengths and are being explored in clinical trials, they each have inherent limitations[34].

For example, peptide vaccines require complex preparation. They are subject to HLA polymorphism and restriction. Additionally, they can be rapidly degraded in the host. Furthermore, they are often less intrinsically immunogenic, requiring the use of adjuvants to increase efficacy[35].

For cell-based vaccines, the processes of generating patient-specific immune cells often require significant expertise and resources. Moreover, tumor cells develop immune evasion mechanisms. The

suppressive effect of the tumor microenvironment (TME) can also impede the efficacy of activated immune cells[25].

Vaccines that are DNA-based have encountered issues including poor immunogenicity. They often require large quantities of genomic material and the use of adjuvants to augment their effectiveness. There remains a risk of DNA integrating into the host genome[36].

For RNA-based vaccines, they suffer from instability in vivo. There is also inefficient delivery of mRNA-based vaccines. Although they generally have higher intrinsic immunogenicity than DNA and pose no risk for host genome integration, their antigenic expression is often transient in nature and may limit effectiveness[37].

Finally, viral vaccines are subject to antiviral immune responses that neutralize the vector, which can hinder the efficacy of repeated vaccinations[38].

Despite the different challenges posed by antigen types and vaccine classes, all cancer vaccines encounter common obstacles in immunotherapy resistance. These include HLA downregulation, lower neoantigen levels, disruptions in signaling pathways, changes in adaptive immunity, and increased innate immune responses. Novel strategies to overcome these barriers and improve vaccine effectiveness are needed[39].

2. Materials and Methods

2.1. TCGA cancer database

The PBK gene expression in tumor and normal samples from The Cancer Genome Atlas (TCGA) was analyzed using the GEPIA2 web portal (http://gepia2.cancer-pku.cn/). Normal tissue gene expression data were obtained from the GTEx portal (https://gtexportal.org/). To verify the expression profiles from TCGA and GTEx, additional gene expression data for colon tumors and paired normal samples were downloaded from the Gene Expression Omnibus (https://www.ncbi.nlm.nih.gov/geo/).

2.2. Kaplan–Meier plotter database analysis

Survival analysis between PBK-high and -low groups was conducted using the Tumor Immune Estimation Resource (TIMER, http://timer.cistrome.org/) web portal across TCGA cancer types. TCGA patient samples were divided into two cohorts based on the 25% cutoff expression values. Overall survival (OS) and disease-free survival (DFS) for the two cohorts were visualized with Kaplan–Meier curves, including hazard ratios (HRs) from the Cox proportional hazards model and log-rank p values.

2.3. Estimation of immune cell enrichment from RNA-seq data

Immune cell infiltration scores were estimated using multiple deconvolution methods from TCGA and CPTAC-2 RNA sequencing data on the TIMER2.0 web portal (http://timer.cistrome.org/). The CIBERSORT algorithm was used for the estimations. The analysis results were visualized using heatmaps or scatter plots created with the R programming language (version 4.1.1, https://www.r-project.org/).

2.4. Epitope prediction and peptide synthesis

The PBK sequences were obtained from GenBank and analyzed for 9-amino acid long peptides that could potentially bind to the HLA-A*0201 molecule using the computer-based epitope prediction programs SYFPEITHI (http://www.syfpeithi.de/) and NetMHCpan-4.0 (https://services.healthtech.dtu.dk/services/NetMHCpan-4.0/). The selected candidate peptides, along with control peptides (NY-ESO1, SLLMWITQV), were synthesized by Peptron (Daejeon, Korea) and purified by HPLC to a purity of over 95%.

2.5. Human cell sources and cell lines

Cryopreserved HLA-A*0201-typed human peripheral blood mononuclear cells (PBMCs) were purchased from ImmunoSpot (Cleveland, OH) and used to evaluate peptide-specific CD8+ T cell

responses. The T2 cells that express HLA-A*02:01 is deficient for the transporter associated with antigen processing (TAP) and is classically used to assess the stability of peptide/HLA-A2 complexes. The T2 cell line was obtained from ATCC. T2 cells were maintained in RPMI 1640 medium with 10% FBS (WELGENE, Korea), 100 IU/ml penicillin, and 100 μg/ml streptomycin (WELGENE, Korea).

2.6. Affinity measurement of peptide for HLA-A*0201

T2 cells were incubated with various concentrations of each peptide and 3 μg/mL human β2m proteins in serum-free RPMI 1640 medium at 37℃ for 16 hours. After incubation, the cells were washed and stained with anti-HLA-A2 mAb and FITC-labeled goat anti-mouse IgG. The expression of HLA-A0201 on T2 cells was determined using flow cytometry (CytoFLEX). For each peptide concentration, the percent mean fluorescence index (% MFI) increase of the HLA-A*0201 molecule was calculated using the following formula: % MFI increase = [(MFI with the given peptide − MFI without peptide) / MFI without peptide] × 100.

2.7. Assessment of peptide/HLA-A*0201 complex stability

T2 cells (10^6/mL) were incubated overnight with 100 μM of each peptide in serum-free RPMI 1640 medium supplemented with 100 ng/mL human β2m at 37°C. They were then washed to remove free peptides and incubated with 10 μg/mL of Brefeldin A (Sigma-Aldrich, USA) for 1 hour to block the expression of newly synthesized HLA-A0201 molecules on the cell surface. After washing, the cells were incubated at 37℃ for 0, 2, 4, 6, or 8 hours. Finally, the cells were stained with anti-HLA-A2 mAb to evaluate the expression of HLA-A*0201 molecules.

2.8. Induction of peptide-specific CTLs

PBMCs from healthy HLA-A*0201 donors were used in this study. CD14+ monocytes were isolated from autologous PBMCs using MojoSort Human CD14 Nanobeads (BioLegend) and cultured in complete RPMI 1640 medium supplemented with 80 ng/mL granulocyte-macrophage colony-stimulating factor (GM-CSF) and 80 ng/mL IL-4 for 5 days. The differentiated monocyte-derived dendritic cells (DCs) were collected and loaded with 20 μg/mL peptide at 37℃ in 5% CO2 for 4 hours. These peptide-loaded DCs were then cocultured with CD8+ T cells at a 1:10 ratio in complete RPMI medium containing 10% FBS. After 24 hours, 5 ng/mL IL-2, 5 ng/mL IL-15, and 10 ng/mL IL-7 (all from Peprotech) were added. Half of the medium was replaced with fresh cytokine-containing media every 3 days. The effector cells were then used to monitor antigen-specific IFN-γ expression and cytotoxicity.

2.9. Interferon-γ ELISPOT assay

A human IFN-γ ELISPOT assay kit was used to determine the number of IFN-γ expressing CTLs. T2 cells, with or without peptide loading, served as target cells. Effector cells were incubated in duplicate for 18 hours at 37℃ with the target cells in a 96-well ELISPOT plate coated with anti-human IFN-γ antibody. Biotinylated antibody, streptavidin-enzyme conjugate, and the enzyme substrate nitroblue tetrazolium were sequentially added to the plates, followed by a 30-minute incubation at room temperature. Images of the spots were captured using an S6 M2 ELISpot reader.

2.10. Cytotoxicity assay

To measure the cytotoxic response of the CTLs induced by target cells with different peptides, T2 cells constitutively expressing luciferase were used. T2 cells, loaded with or without peptide, served as target cells. PBK #3-CTLs and PBK #8-CTLs were used as the effector cells, with an irrelevant peptide, NY-ESO-1, as a negative control. T2 cells were loaded with or without peptide for 4 hours at 37℃ in 5% CO2 and washed three times. Target cells were then cocultured with effector cells at different ratios (E:T = 10:1, 20:1, 40:1) in 96-well U-bottom plates. After incubation for 4 hours at 37℃ in 5% CO2, the killing activity was measured by assessing the luciferase activity of viable cells. Luminescent signals emitted from the cell lysates were quantified using the Luciferase Assay System (Enzynomics) according to the manufacturer's instructions.

2.11. Plasmids

The full-length mouse PBK gene was synthesized and cloned into the pMSCV-puro vector (Clontech). The pMSCV-PBK(K63A/K64A) mutant was generated using a QuikChange site-directed mutagenesis kit (Stratagene) according to the manufacturer's instructions. All construct sequences were verified by Sanger sequencing. PBK in CT26 cells was knocked out via CRISPR/Cas9. The guide sequences (PBK: 5′-TTGCTTTGCACATGGCCAGA-3′) were cloned into pX330-mCherry vector (Addgene plasmid #98750). CT26 cells were transfected with sgRNA expressing plasmid, and the resulting transfected cells were single cell subcloned. PBK expression in the resulting cells was confirmed by western blot analysis.

2.12. Retrovirus production and stable cell line generation

For retroviral production, PLAT-E cells were seeded at a density of 3.3 × 10^6 cells per 100 mm dish. The following day, pMSCV-PBK WT and pMSCV-PBK(K63A/K64A) plasmids were individually transfected into PLAT-E cells using Lipofectamine 3000 transfection reagent

(ThermoFisher Scientific). After 24 hours, the medium was replaced with 10 mL of DMEM supplemented with 10% FBS, and the supernatant was collected the next day. MC38 cells were then infected with the retrovirus-containing supernatants and screened with puromycin. PBK expression in the resulting cells was confirmed by western blot analysis.

2.13. Western blot

The CT26 and CT26-PBK KO cells were lysed in SDS sample buffer containing 60 mM Tris HCl, 2% SDS, 10% glycerol, and 100 mM dithiothreitol. Cell lysates were resolved by SDS-PAGE and immunoblotted with the indicated antibodies. For immunoblotting, primary antibodies against PBK (BD) and β-actin (Santa cruz) were purchased.

2.14. The analysis of tumor infiltrating lymphocytes

Mouse tumors were dissected and digested with collagenase IV (250 units/ml, Worthington Biochemical Corporation) and DNase I (100 μg/ml, Roche Diagnostics GmbH) in HBSS using a gentleMACS dissociator (Miltenyi Biotec). TILs were enriched through Ficoll–Hypaque (MilliporeSigma) gradient centrifugation, resulting in the recovery of single cells. Cell viability was then assessed using trypan blue exclusion.

2.15. FACS analysis

Mouse single cells were blocked with human TruStain FcX™ (BioLegend) and anti-mouse CD16/32 (BioLegend), respectively, and then stained with the indicated antibodies in fluorescence-activated cell sorter (FACS) buffer (PBS containing 2% FBS and 0.1% sodium azide) for 20 min at 4°C. Dead cells were excluded using Zombie NIR Fixable viability dye (BioLegend). For intracellular staining, cells were stained with antibodies to surface markers and then fixed and permeabilized with Foxp3 / Transcription Factor Fix/Perm Concentrate (TONBO), followed by staining with indicated antibodies diluted in Flow Cytometry Perm Buffer (TONBO). The following fluorescent dye-conjugated anti-human antibodies were used: anti-TCRb (H57-597), anti-CD4 (GK1.5), anti-CD8 (53-6.7), anti-CD45 (30-F11), anti-Granzyme B (QA16A02), anti-Ki-67 (11F6), anti-Foxp3 (FJK-16s), anti- MHC-II (I-A/I-E)(M5/114.15.2), anti-PD-L1(10F.9G2), anti-PVR(SKIL4) (purchased from BioLegend, TONBO and Invitrogen). The acquisition of FACS data was performed on a CytoFLEX flow cytometer (Beckman Coulter, Brea, CA) and analyzed with FlowJo software (v.10.5.3, TreeStar). The automated analysis of multi-parameter flow cytometry data was subjected to the t-SNE (t-Distribution Stochastic Neighbor Embedding)-CUDA algorithm provided by Cytobank software (Beckman Coulter, Brea, CA).

An equal number of cells (50,000 cells) from each FACS file were used to generate t-SNE plots.

2.16. Syngeneic tumor model

CT26 cells were obtained from the Legochem, Korea and maintained as recommended by the Legochem. For tumor challenge, CT26 cells were resuspended in HBSS solution (Welgene, Korea) and subcutaneously injected into the left flank of BALB/c mice. Tumor volumes were calculated as (length × width2)/2. Tumors were analyzed by flow cytometry at 11 days after implantation.

2.17. Statistical analysis

Statistical analysis was performed using GraphPad Prism. Statistical significance was determined with two-tailed unpaired Student's t-test. P values < 0.05 were considered statistically significant (*< 0.05, **< 0.01, ***< 0.001, and **** < 0.0001).

3. Results

3.1. PBK expression in tumor and normal tissue samples

The expression pattern of PBK was thoroughly analyzed in both normal tissues and various tumor tissues to understand its distribution and potential role in different cellular environments. As shown in **Figure 1A**, the analysis revealed that PBK is highly expressed in testis. This suggests a possible role for PBK in the specialized functions or high cellular turnover associated with these tissues. Conversely, PBK exhibits low expression in brain, breast, liver, and other normal tissues, indicating a more restricted role or regulation in these contexts. To further explore the differential expression of PBK, a comparison of PBK mRNA levels between cancerous and normal tissues was conducted using data from The Cancer Genome Atlas (TCGA) database. This comparison revealed that PBK is significantly overexpressed in most tumor tissues ($p < 0.05$), with the notable exceptions of SKCM (skin cutaneous melanoma), THYM (thymoma), and READ (rectum adenocarcinoma), as shown in **Figure 1B**. This pattern suggests that PBK may play a varying role in different tumor types and may not be universally overexpressed in all cancers. These analyses demonstrate that PBK is aberrantly overexpressed in most tumor types, suggesting its potential role as a biomarker or therapeutic target in cancer. The variable expression patterns observed across different cancers highlight the complexity of PBK regulation and its possible involvement in diverse oncogenic pathways.

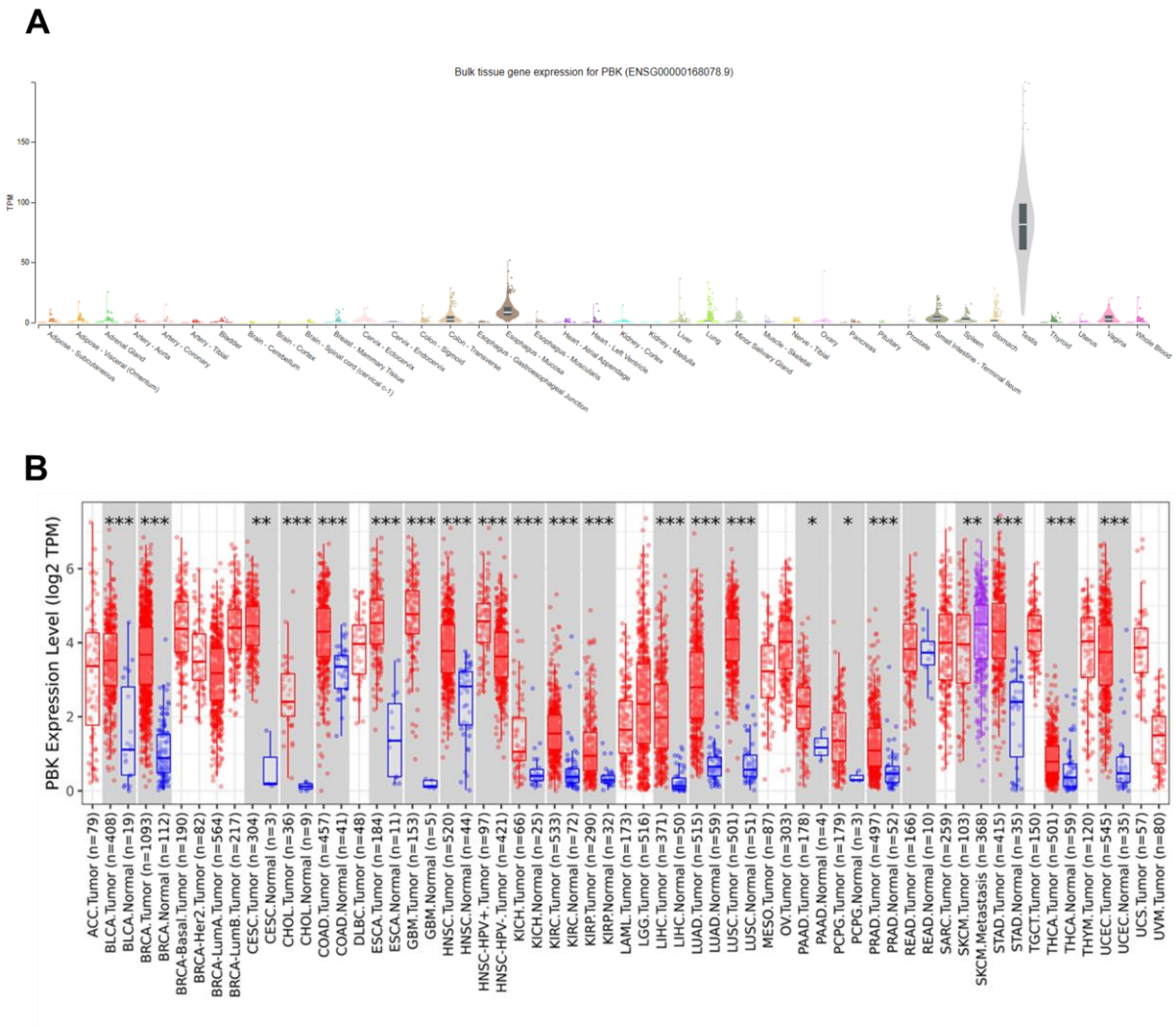

Figure 1. PBK levels in tumor and normal tissue samples

(A) Analysis of PBK gene expression was conducted in each normal tissue downloaded from the GTEx web portal. **(B)** A comprehensive examination of PBK gene expression across various cancer types was conducted utilizing the GEPIA2 website. Tumor tissues (T, indicated by red dots) represent TCGA tumors, while normal tissues (N, indicated by green dots) represent TCGA normal tissues. Expression values are displayed as log-normalized transcripts per million (TPM) with median values indicated by horizontal black bars. The color variations of the cancer type abbreviations (red and green) signify significant differences in PBK gene expression levels in these tumor tissues compared to normal tissues. TCGA abbreviations: ACC, adrenocortical carcinoma; BLCA, bladder urothelial carcinoma; BRCA, breast invasive

carcinoma; CESC, cervical squamous cell carcinoma and endocervical adenocarcinoma; CHOL, cholangiocarcinoma; COAD, colon adenocarcinoma; DLBC, diffuse large B-cell lymphoma; ESCA, esophageal carcinoma; GBM, glioblastoma multiforme; HNSC, head and neck squamous cell carcinoma; KICH, kidney chromophobe; KIRC, kidney renal clear cell carcinoma; KIRP, kidney renal papillary cell carcinoma; LAML, acute myeloid leukemia; LGG, lower grade glioma; LIHC, liver hepatocellular carcinoma; LUAD, lung adenocarcinoma; LUSC, lung squamous cell carcinoma; MESO, mesothelioma; OV, ovarian serous cystadenocarcinoma; PAAD, pancreatic adenocarcinoma; PCPG, pheochromocytoma and paraganglioma; PRAD, prostate adenocarcinoma; READ, rectum adenocarcinoma; SARC, sarcoma; SKCM, skin cutaneous melanoma; STAD, stomach adenocarcinoma; TGCT, testicular germ cell tumors; THCA, thyroid carcinoma; THYM, thymoma; UCEC, uterine corpus endometrial carcinoma; UCS, uterine carcinosarcoma; UVM, uveal melanoma.

3.2. The expression levels of PBK are correlated with patient prognosis

The prognostic value of PBK was examined in several cancers, including colon adenocarcinoma (COAD), head and neck squamous carcinoma (HNSC)-human papillomavirus (HPV)+, adenoid cystic carcinoma (ACC), lung adenocarcinoma (LUAD), low-grade gliomas (LGG), Kidney renal papillary cell carcinoma (KIRP), malignant mesothelioma (MESO), pancreatic adenocarcinoma (PADD), sarcoma (SARC), kidney renal clear cell carcinoma (KIRC) and Thymoma (THYM) within the TCGA cohort. High expression levels of PBK were associated with poorer overall survival (OS) in ACC (OS HR = 2.5, p = 7.98e-05), LUAD (OS HR = 1.23, p = 0.00202), LGG (OS HR = 1.6, p = 1.26e-06), KIRP (OS HR = 1.5, p = 0.00538), MESO (OS HR = 1.61, p = 0.000168), PADD (OS HR = 1.3, p = 0.0133), SARC (OS HR = 1.22, p = 0.0515) and KIRC (OS HR = 1.13, p = 0.0821). Conversely, elevated PBK expression correlated with a better prognosis in COAD (OS HR = 0.31, p = 0.0026), HNSC-HPV+ (OS HR = 0.601, p = 0.00513) and THYM (OS HR = 0.3, p = 0.0244) as shown in **Figure 2**. The implications of these results suggest that PBK expression levels could serve as potential prognostic markers in specific cancer types, providing valuable insights into patient prognosis and

aiding in the development of targeted therapeutic strategies. However, the varying significance across different cancers highlights the complexity of PBK's role and suggests the need for further investigation to fully understand its prognostic potential in diverse oncological contexts. Importantly, the analysis indicates that PBK expression is associated with a favorable prognosis in patients with colon cancer.

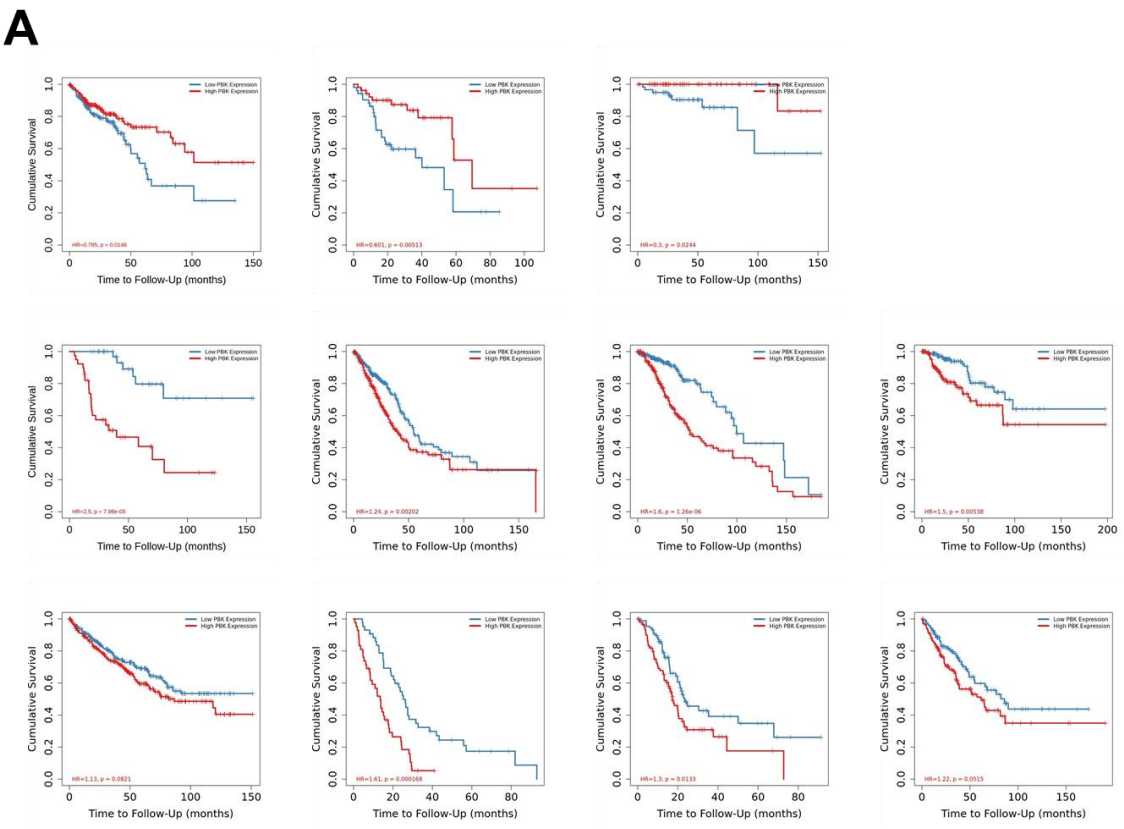

Figure 2. Patient prognosis is associated with PBK expression levels

PBK expression is associated with a positive prognosis in colon cancer. Kaplan-Meier curves were generated to assess overall survival (OS) across different solid tumors based on PBK expression levels.

3.3. Correlation between PBK expression and the antitumor activity of tumor-infiltrating immune cells in colon cancer

Immune cell infiltration is a crucial factor for evaluating tumor-immune interactions and their impact on overall survival (OS) in colon cancer[40]. To investigate whether the favorable prognosis of PBK-high colon cancer is linked to an increased presence of antitumor immune cells in the tumor microenvironment (TME), the cellular composition of intratumoral immune infiltrates was analyzed.

This was done using bulk RNA-sequencing data from TCGA colon cancer samples, employing a deconvolution algorithm, CIBERSORT[41]. The analysis revealed a positive correlation between PBK expression and the infiltration levels of antitumor immune cells, such as activated CD4+ T cells, CD8+ T cells, activated/resting natural killer (NK) cells, and M1 macrophages. Additionally, immunosuppressive protumor immune cells, like regulatory T (Treg) cells and M0 macrophages, showed limited infiltration in PBK-high colon cancer patients (**Figure 3A**). In order to gain insights into the functional attributes of infiltrating immune cells within PBK-high colon cancer, an analysis was conducted to examine PBK mRNA levels in relation to granzyme A, granzyme B, and IFN-γ expression in CD8A cells as indicators of cytotoxicity. The analysis revealed significant positive correlations between PBK expression and the GZMA/CD8A ratio ($R = 0.15$, $p = 0.00081$), the GZMB/CD8A ratio ($R = 0.13$, $p = 0.0024$), and the IFNG/CD8A ratio ($R = 0.25$, $p = 8.6 \times 10{-}9$). These findings suggest that elevated levels of PBK are associated with enhanced cytotoxic activity of CD8+ T cells (**Figure 3B**). Given that PBK expression not only correlates with the degree of infiltration by CD8+ cells but also with their cytotoxic functions, it prompts consideration as to whether PBK expression might represent an antitumor response by CD8+ T cells. These results underscore the link between high PBK expression and a favorable immune cell profile within TME of colon cancer, potentially contributing to an improved prognosis for patients.

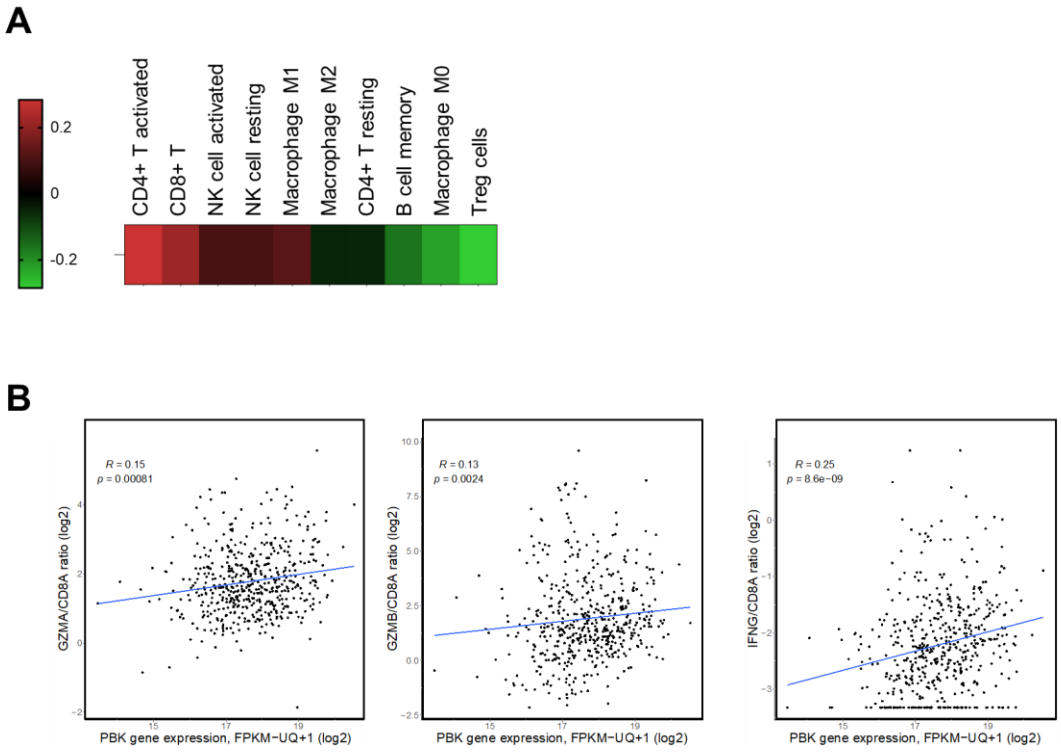

Figure 3. Association between PBK expression and the antitumor activity of immune cells infiltrating tumors in colon cancer

The relationship between PBK expression and immune cell infiltration in colon cancer was examined. (A) The correlation between deconvolution analysis results and PBK expression in TCGA colon cancer samples was illustrated using a heatmap plot depicting Spearman's correlation coefficients. (B) The scatter plots illustrate the relationship between the expression of CD8A-normalized cytotoxic T-cell marker genes and PBK expression. Statistical significance was determined by evaluating the Spearman's correlation p value.

3.4. Identification of PBK peptides that bind to HLA class I molecules

Cancer/testis antigens (CTA) are characterized by their predominant expression in various types of cancer while being undetectable in normal tissues, except for germ cells in the testis. The expression of CTAs in the placenta or testis does not typically lead to T-cell activation due to the very low expression

of MHC class I molecules in these tissues. While normally restricted to the male testis, CTAs are aberrantly overexpressed in cancer stem-like cells and various cancers, making them promising targets for cancer immunotherapy[42]. For instance, the increased expression of CTAs like MAGE-A2 enhances tumor recognition by T cells, aiding in the elimination of esophageal cancer cells. MAGE-A-derived peptides are presented on the cell surface by MHC class I molecules, allowing CD8+ T cells to recognize and target cancer cells, thereby highlighting CTAs as potential targets for anticancer immunotherapy[43]. PBK expression is typically restricted to the testis, but it is significantly overexpressed in the majority of cancer tissues. Given that high PBK expression in colon cancer is associated with improved prognosis and increased infiltration of cytotoxic immune cells, PBK emerges as a promising molecular target for colon cancer therapy. This could be achieved through cancer vaccine-mediated immunotherapy and/or the inhibition of PBK-specific kinase function. The sequence of PBK comprises 333 amino acid residues (Accession number NP_001265874.1). (**Figure 4A**) Initially, five 9-mer peptides were chosen based on AA anchor residues crucial for binding to HLA-A2 molecules, alongside the utilization of two predictive algorithms, NetMHCpan-4.0 and SYFPEITHI. The NetMHCpan algorism utilizes artificial neural networks (ANNs) trained on a combination of over 180,000 quantitative binding data and MS-derived MHC-eluted ligands[44]. The SYFPEITHI score, developed by Hans-Georg Rammensee's lab (http://www.syfpeithi.de/), indicates a potential HLA-A2 epitope with a score higher than 21[45]. The predictions were not entirely consistent across the two algorithms. Peptides recommended as binders by any one of the predictive algorithms were included for further analysis.

3.5. In vitro induction of PBK peptide-Specific CTLs

A T2 cell peptide-binding test was employed to evaluate the binding ability of the in silico-designed PBK peptides to HLA-A*02:01 molecules. The T2 cell line, which expresses HLA-A*02:01 but lacks the transporter associated with antigen processing (TAP), is traditionally used to examine the stability

of peptide/HLA-A2 complexes. Peptide binding to HLA-A2 molecules can enhance the expression of HLA-A0201 molecules. High-affinity peptides, in particular, can significantly upregulate HLA-A0201 compared to low-affinity peptides, leading to increased stabilization of the complex on the T2 cell surface. As shown in **Figure 4B**, PBK peptides #1, #3, #4, #6, #8, and #9 induced a strong increase in cell surface HLA-A*02:01 stabilization compared to PBK peptides #2, #5, and #7. These findings indicate that the high binding scores of PBK peptides correlate with their high affinity for HLA-A*02:01 molecules. To further investigate the stability of the peptide/HLA-A2 complexes, the relative stability of the nine peptide/HLA-A2 complexes was determined by measuring their dissociation time (t 1/2) over an 8-hour period. Representative dissociation curves for the PBK peptides are depicted in **Figure 4C**. Among the nine PBK peptides, five (#1, #3, #6, #8, and #9) demonstrated a t 1/2 exceeding 6 hours. This indicates that these peptides exhibit both high binding affinity and low off-rate stability. Therefore, the results confirm that PBK peptides #1, #3, #6, #8, and #9 not only have high binding affinity but also form stable peptide/HLA-A2 complexes.

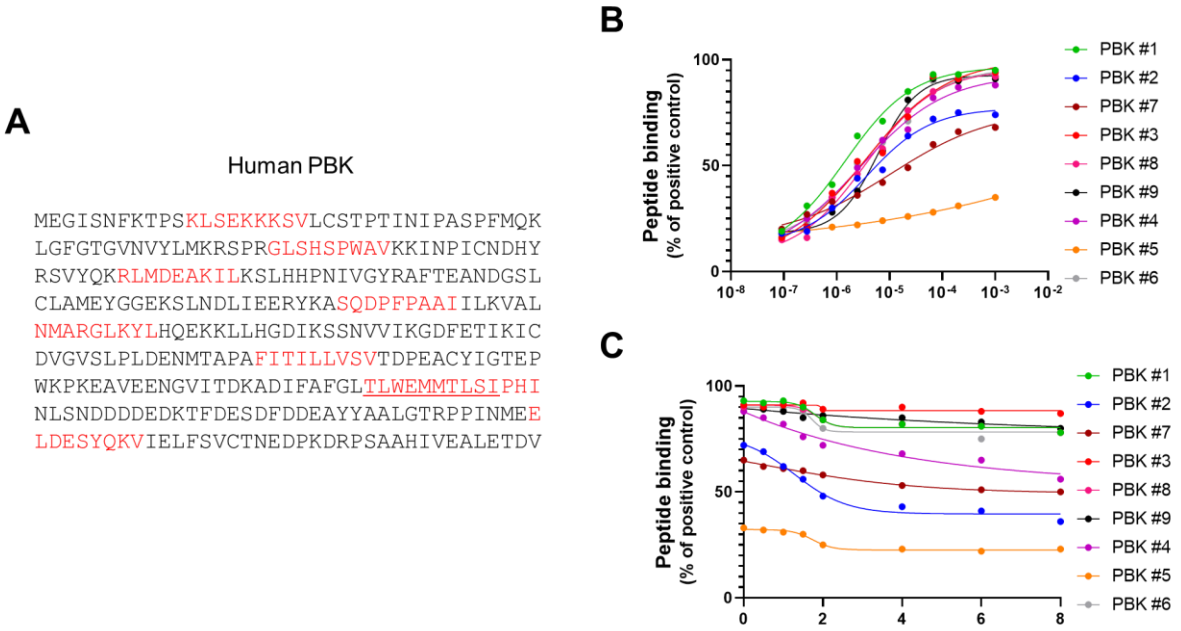

Figure 4. Identification of PBK peptides binding to HLA class I molecules

(A) PBK protein sequence

(B) The binding affinity of the 9 predicted peptides for the HLA-A0201 molecule was assessed. T2 cells were exposed to specified concentrations of the peptides in serum-free RPMI 1640 medium supplemented with 3 μg/mL human β2m at 37°C for 16 hours. Subsequently, the cells were labeled with anti-HLA-A2 monoclonal antibody, and the expression of HLA-A0201 on T2 cells was evaluated using flow cytometry.

(C) Off-rate curves for the 9 predicted peptides. T2 cells were exposed to the 9 predicted peptides in the presence of Brefeldin A. After 1 hour, the cells were washed and placed in serum-free medium at 37°C. Surface levels of HLA-A2 molecules were assessed by flow cytometry at the beginning of this incubation period.

3.6. PBK reactive CTLs can lyse peptide-pulsed T2 target cells

To investigate whether these candidate epitope peptides can stimulate the generation of peptide-specific CD8+ cytotoxic T lymphocytes (CTLs) in vitro, peripheral blood mononuclear cells (PBMCs) were collected from individuals with the HLA-A*0201 allele. The procedure involved using dendritic cells (DCs) to prime naive anti-PBK CD8+ T cells present in the PBMCs from HLA-A2+ donors. These dendritic cells, once matured and treated with the PBK peptides, were co-incubated with autologous CD8+ T cells to initiate the priming process.

The antigen specificity of the peptide-induced CTLs was assessed by measuring the secretion of IFN-γ in response to target cells. For this purpose, T2 cells pulsed with nine different PBK peptides were used as targets in IFN-γ ELISPOT and cytotoxicity assays. The IFN-γ ELISPOT assay revealed that PBK #3 and PBK #8 peptides significantly primed more epitope-specific CTLs compared to the other peptides (**Figure 5**). The frequencies of IFN-γ producing T cells induced by PBK #3 and PBK #8 peptides were notably higher than those induced by the other PBK peptides.

The cytotoxic activity of the antigen-specific CTLs was further evaluated using a cytotoxicity assay. The results demonstrated that T2 cells loaded with the PBK #3 peptide could be effectively lysed by the CTLs induced by PBK #3. However, these CTLs were unable to lyse T2 cells loaded with either PBK #8 or NY-ESO-1 peptides at any effector-target ratio (**Figure 6A**). Similarly, CTLs induced by PBK #8 efficiently lysed T2 cells loaded with the PBK #8 peptide, but did not affect T2 cells loaded with irrelevant peptides (**Figure 6B**). These findings illustrate that PBK #3 and PBK #8 peptides can effectively induce antigen-specific CTLs in vitro, highlighting their potential for targeted immunotherapy.

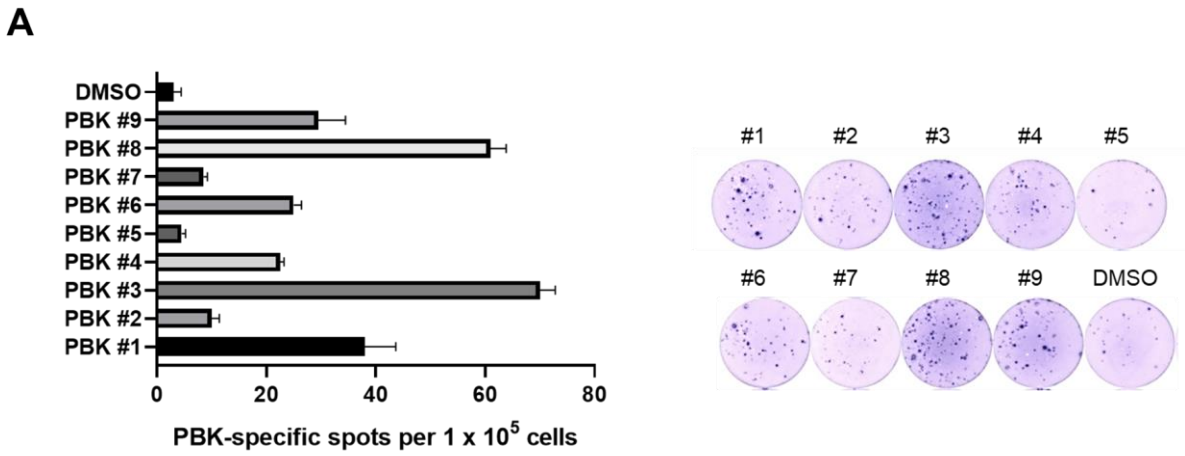

Figure 5. Induction of PBK peptide-specific CTLs in vitro

Identification of HLA-A2-restricted PBK-derived peptide that activates CD8+ T cells. A ELISPOT was used to detect IFN-γ secretion by peptide-induced T cells.

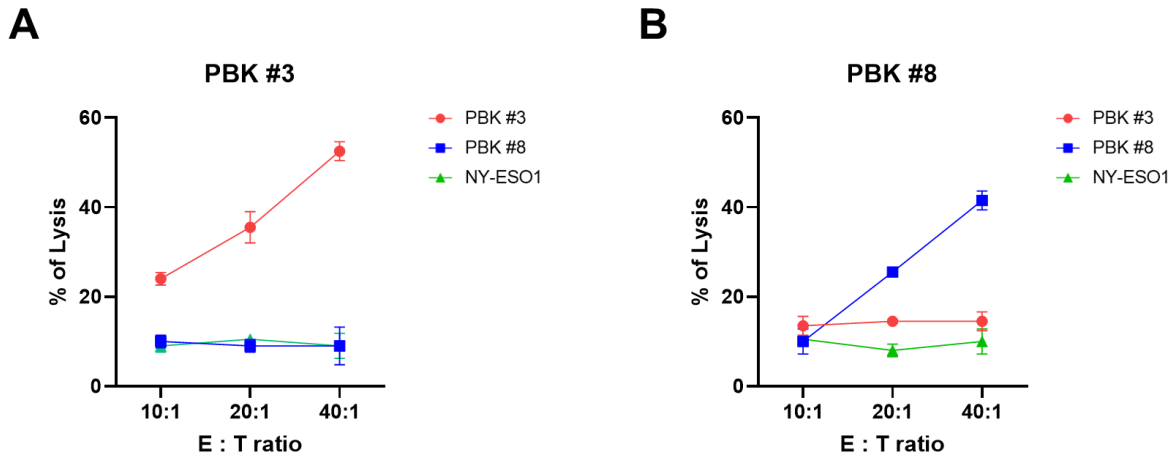

Figure 6. PBK-responsive CTLs have the capability to induce lysis of T2 target cells pulsed with the peptide

(A) Human CTLs specific to the PBK #3 peptide were tested for their responsiveness towards T2 cells loaded with either the corresponding peptide or control PBK #8 peptide at various effector to target

ratios using the luciferase activity assay. An irrelevant NY-ESO-1 peptide served as the negative control.

(B) The responsiveness of human CTLs targeting the PBK #8 peptide was assessed by exposing them to T2 cells loaded with either the PBK #8 peptide or a control PBK #3 peptide at different effector-to-target ratios using the luciferase activity assay. An irrelevant NY-ESO-1 peptide served as the negative control.

3.7. Analysis of PBK expression and its impact on cancer cell proliferation and immunogenicity

In order to develop a CD8+ T cell-based therapeutic vaccine targeting cancer cells that express PBK, a series of experiments were conducted to identify peptides that are effectively presented by HLA-A*0201. The PBK peptides were selected for their potential to be recognized by the immune system, thereby enhancing anti-tumor immune responses. It was confirmed through various assays that the identified peptides can significantly enhance the activation and cytotoxicity of CD8+ T cells. Furthermore, in order to evaluate the feasibility of PBK-targeted therapeutic approaches, a research was undertaken to establish a mouse model system. This model will serve as a preclinical platform to test the therapeutic vaccine, assess its immune response, and optimize its potential for future clinical applications.

In various mouse colon cancer cell lines, PBK expression was examined, and high PBK expression in the CT26 cell line was confirmed through Western blotting. Additionally, PBK expression was evaluated in various mouse tissues to understand its distribution across different tissue types. It was confirmed that PBK was not expressed in any of the assessed tissues, highlighting its specific expression

in certain cancer cells and not in normal tissues (**Figure 7A**).

To determine if PBK gene deletion affects the propagation of cancer cells, the PBK gene was removed from CT26 cells using the CRISPR-Cas9 technique. This gene-editing approach allowed for precise and efficient knockout of PBK. From several clones generated, clone #1, in which PBK was completely removed, was selected for further experiments (**Figure 7B**).

To verify whether PBK knockout affects the in vitro proliferation of CT26 cells, cell growth was assessed using the CellTiter-Glo assay, a luminescent assay that measures cellular ATP as an indicator of cell viability and proliferation. The proliferation assay results showed that CT26 and CT26-PBK KO cells grew at similar rates, indicating that PBK does not influence cell growth under in vitro conditions (**Figure 8A**). This finding was significant as it suggested that the absence of PBK does not impair the basic proliferative capacity of these cancer cells.

Next, the impact of PBK abrogation on the antigenicity of CT26 cells was examined. Immunogenicity refers to the ability of a cell to provoke an immune response. It is known that increased expression of MHC molecules enhances antigen presentation to T cells, thereby increasing the antigenicity of cancer cells. Flow cytometry analysis of MHC-I and MHC-II expression revealed that both CT26 and CT26-PBK KO cells exhibited similar levels of MHC-I and MHC-II proteins on their cell surfaces (**Figure 8B**). These results suggest that PBK abrogation may not affect the antigenicity of CT26 cells

Additionally, the expression of the immune checkpoint ligands PD-L1 and PVR in CT26 and CT26-PBK KO cells was examined. Immune checkpoint molecules play crucial roles in the regulation of immune responses, and their expression can influence the ability of the immune system to recognize and attack cancer cells. A detailed comparison between CT26 PBK KO and CT26 cell lines showed similar levels of PD-L1 and PVR expression in both cell types (**Figure 8B**). These findings indicate that PBK abrogation does not affect the expression of immune checkpoint molecules.

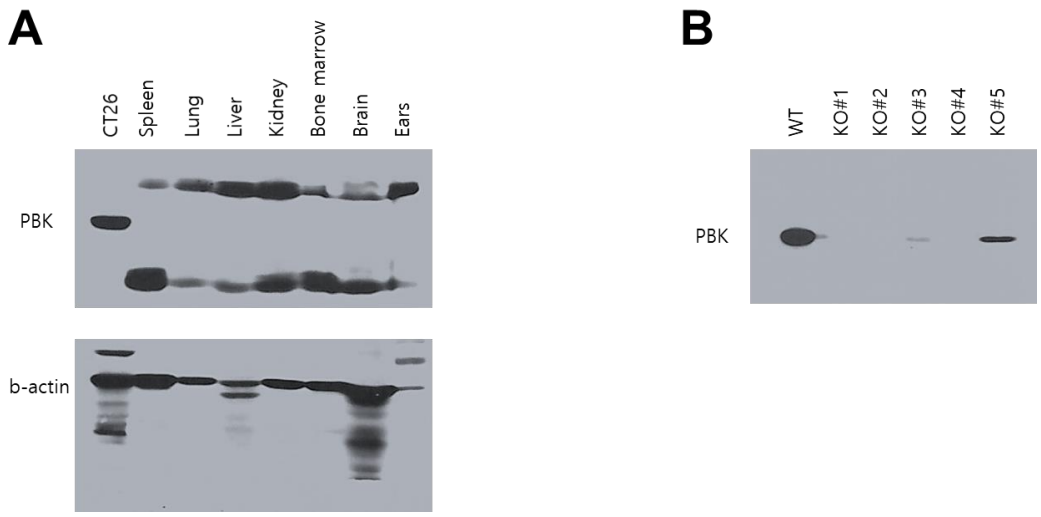

Figure 7. Expression of PBK in mouse tissues and CT26 cells and generation of PBK KO CT26 cells

(A) Western blot analysis of PBK expression in the CT26 cell line and various mouse tissues. Total protein was separated by SDS-PAGE and transferred to nitrocellulose membranes for Western blotting. The PBK protein was detected using an anti-PBK antibody, with β-actin protein levels shown as a loading control.

(B) The PBK expression in various PBK knockout candidate cell clones was examined using Western blotting with anti-PBK antibody.

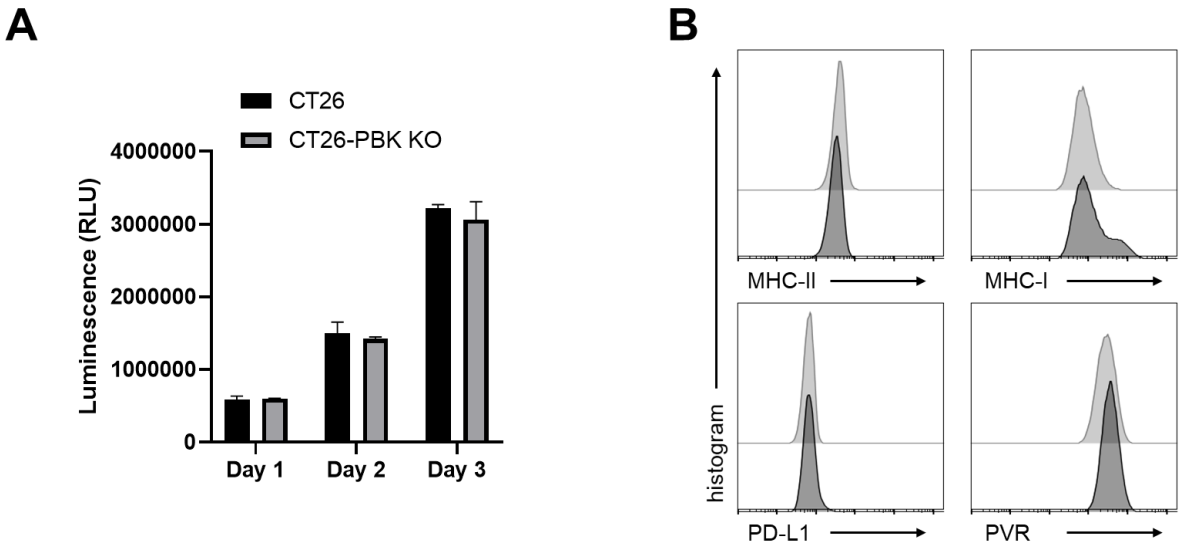

Figure 8. The in vitro proliferation and immunogenicity of CT26 cells are unaffected by PBK abrogation

(A) The proliferation of CT26 and CT26-PBK KO cells was assessed using the CellTiter-Glo Luminescent Cell Viability Assay, which measures luminescent signals correlated with cellular ATP levels.

(B) The expression of MHC-I (I-Ad), MHC-II (I-A/I-E), PD-L1, and PVR in CT26 and CT26-PBK KO cells was analyzed using flow cytometry.

3.8. Evaluation of PBK targeting therapeutic approaches in mouse preclinical models

To assess the impact of PBK abrogation on cancer cell growth in vivo, CT26 and CT26-PBK KO cell lines were implanted into BALB/c mice. Monitoring the growth of the transplanted tumors revealed a reduction in the growth of CT26 cells lacking PBK (**Figure 9**).

Since PBK deficiency did not affect the growth of CT26 cells in vitro, the analysis of tumor infiltrating lymphocytes (TILs) was conducted to determine whether extrinsic factors could inhibit the in vivo growth of the CT26-PBK KO cells (**Figure 10**). The composition and activation of immune

cells within tumor tissues were evaluated to assess whether the immune system influenced the inhibition of in vivo propagation of CT26-PBK KO cells.

The analysis of TILs using flow cytometry showed a significant increase in the number of CD4+ T cells, CD8+ T cells, and Treg cells in TILs isolated from mice transplanted with CT26-PBK KO cells compared to those with CT26 cells (**Figure 11A**). Interestingly, it was observed that the expression of granzyme B in CD8+ T cells isolated from the mice with CT26-PBK KO cells significantly increased (**Figure 11B**). Granzyme B is a critical enzyme involved in the cytotoxic activity of CD8+ T cells, indicating that PBK deficiency enhances the cytotoxic potential of these immune cells against cancer cells. This heightened cytotoxicity likely contributes to the increased killing of cancer cells by the immune system in the context of PBK-deficient tumors.

Interestingly, there was no difference in the expression of Ki-67, a marker for cell proliferation, in CD8+ and CD4+ T cells between the two groups of mice (**Figure 11B**). This indicates that PBK deficiency does not affect the proliferation of these T cells. Therefore, the observed increase in the number of T cells in the tumor microenvironment is likely due to the recruitment of T cells rather than their proliferation.

Overall, these results highlight the role of PBK in modulating the immune response within the tumor microenvironment. The increased infiltration and cytotoxic activity of T cells in PBK-deficient tumors underline the potential for targeting PBK in cancer immunotherapy to enhance the anti-tumor immune response.

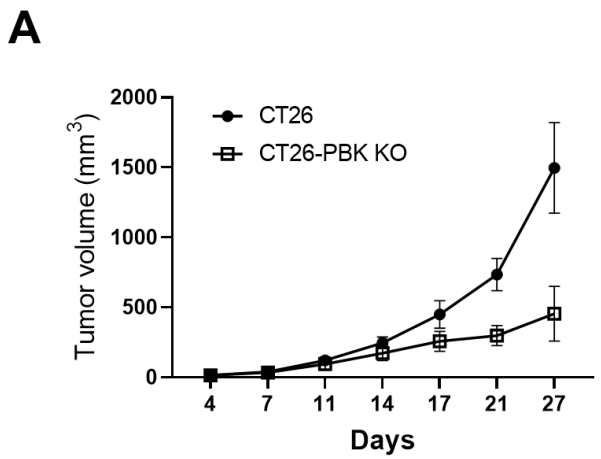

Figure 9. The in vivo growth of CT26 cells is hindered by PBK deficiency

To establish a murine colon cancer model with CT26 cells, 1×10^6 cells were subcutaneously implanted into the right flank of female BALB/c mice. Tumor growth was monitored using vernier calipers, and the mean tumor volume was calculated using the specified formula.

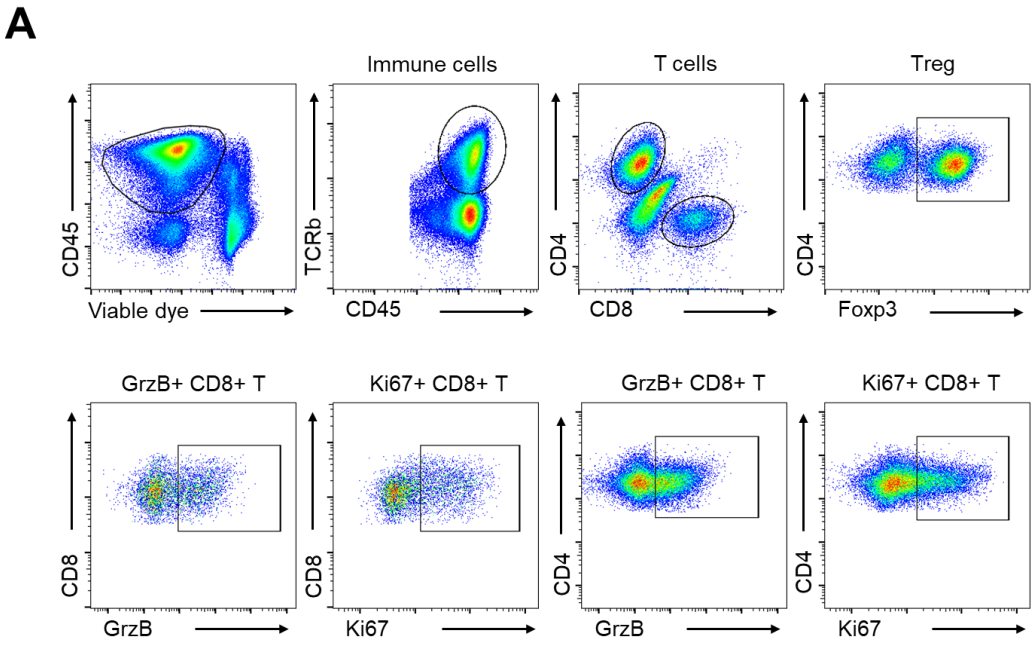

Figure 10. A representative flow cytometry gating strategy for analyzing tumor-infiltrating lymphocytes in mice harboring CT26 cells

TILs are stained with a Live/Dead discriminator, CD45, TCRb, CD4, CD8, Foxp3, granzyme B (GrzB), and Ki67. With this strategy, the first gate excludes non-lymphocyte populations based on CD45 expression. Following this, TCRb+ live cells are selected. CD8+ T cells are defined as CD45+TCRb+CD8+CD4-. CD4+ T cells are defined as CD45+TCRb+CD8-CD4+. Treg cells are defined as CD45+TCRb+CD8-CD4+Foxp3+. The expression of GrzB and Ki67 in T cells was measured via intracellular staining.

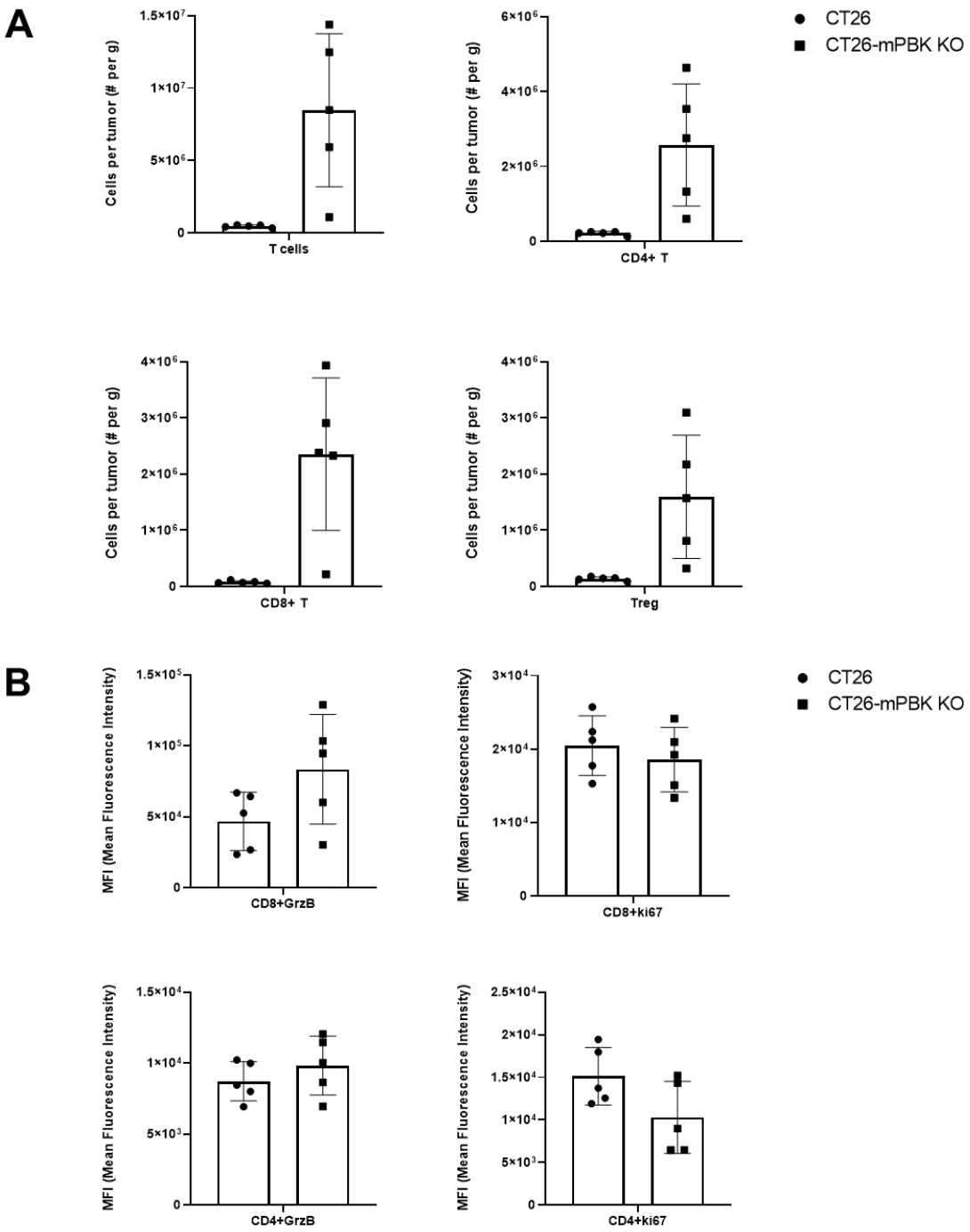

Figure 11. The impact of PBK deficiency on T cell infiltration in the tumor microenvironment and PBK deficiency in CT26 tumors enhances activation of CD8+ T cells within the tumor tissue

(A) Tumor tissues from Balb/c mice bearing CT26 or CT26 PBK KO tumors were harvested, dissociated into single-cell suspensions, and analyzed for immune cell composition using flow cytometry. The absolute number of CD3+ T cells, CD8+ T cells, CD4+ T cells, and Treg cells per tumor weight was quantified.

(B) The levels of granzyme B (GrzB) and Ki67 expressed in T cells isolated from tumor tissues were measured using flow cytometry.

4. Discussion

The analysis of PBK expression in normal and tumor tissues reveals significant insights into its potential role. PBK is predominantly expressed in testis, suggesting involvement in high cellular turnover processes like spermatogenesis. In contrast, low PBK expression in brain, breast, liver, and other normal tissues indicates a limited role in these areas, implying tight regulation of PBK activity. Comparison of PBK mRNA levels between cancerous and normal tissues from the TCGA database shows significant overexpression of PBK in most tumors, highlighting its potential as a biomarker and therapeutic target. Exceptions include SKCM, THYM, and READ, suggesting PBK's role is not universal across all cancers. The widespread overexpression of PBK in tumors suggests its involvement in oncogenic processes such as cell proliferation and survival. Given its limited expression in normal tissues, targeting PBK in cancers could minimize side effects. The variability in PBK expression across cancers underscores the complexity of its regulation and involvement in different oncogenic pathways. The prognostic significance of PBK expression varies across different cancers within the TCGA cohort. High PBK levels are linked to poorer overall survival in ACC, LUAD, LGG, KIRP, MESO, PADD, SARC, and KIRC. This suggests that elevated PBK may contribute to more aggressive tumor behavior in these cancers. In contrast, high PBK expression correlates with better prognosis in COAD, HNSC-HPV+, and THYM. These findings highlight the complexity of PBK's role in cancer prognosis, emphasizing the need for further research to understand its mechanisms in different cancer types.

In colon cancer, the association with improved prognosis suggests potential therapeutic targets, underscoring the importance of tailored treatment approaches based on PBK expression profiles. The investigation revealed that higher PBK expression in colon cancer correlates with increased infiltration of antitumor immune cells, such as activated CD4+ T cells, CD8+ T cells, activated/resting natural killer (NK) cells, and M1 macrophages. This suggests a robust antitumor immune response in PBK-high tumors. In contrast, immunosuppressive cells like regulatory T (Treg) cells and M0 macrophages were less prevalent in these tumors, indicating a less favorable environment for tumor growth. Additionally, the functional analysis of immune cells in PBK-high tumors showed significant positive correlations between PBK expression and markers of cytotoxicity, including granzyme A, granzyme B, and IFN-γ in CD8+ T cells. This enhanced cytotoxic activity suggests that PBK not only attracts more immune cells but also enhances their tumor-killing functions. These findings indicate that PBK expression could be a marker of a strong antitumor immune response, contributing to the improved prognosis observed in patients with high PBK expression.

The concept of cancer/testis antigens (CTAs) has emerged as a promising avenue for cancer immunotherapy due to their unique expression patterns. CTAs, typically silent in normal tissues except for the male testis, become overexpressed in various cancers, offering potential targets for immune-based therapies. This selective expression allows for the recognition of cancer cells by the immune system without inducing autoimmunity. The observed correlation between high PBK expression in colon cancer and favorable prognosis, along with increased infiltration of cytotoxic immune cells, underscores its potential as a therapeutic target in colon cancer therapy. Strategies such as cancer vaccine-mediated immunotherapy could exploit this association for therapeutic benefit.

The identification of PBK peptides capable of binding to HLA class I molecules represents a critical step towards developing targeted immunotherapies. By leveraging predictive algorithms and analyzing binding affinities, potential epitopes for immunotherapeutic interventions can be identified. Although prediction algorithms may show variability, the inclusion of peptides recommended by at least one algorithm ensures comprehensive coverage and enhances the likelihood of identifying functional epitopes. The assessment of peptide binding to HLA molecules is crucial for understanding antigen presentation and the subsequent immune response. In this study, the T2 cell peptide-binding assay was utilized to evaluate the binding capacity of in silico-designed PBK peptides to HLA-A*02:01 molecules. The T2 cell line, which lacks the transporter associated with antigen processing (TAP), serves as a valuable model for examining the stability of peptide/HLA-A2 complexes. The results revealed that certain PBK peptides, particularly #1, #3, #4, #6, #8, and #9, induced a significant increase in cell surface HLA-A*02:01 stabilization compared to others. This observation suggests that peptides with higher binding scores tend to exhibit greater affinity for HLA-A*02:01 molecules, leading to enhanced stabilization of the complex on the cell surface. Furthermore, the study investigated the stability of the peptide/HLA-A2 complexes by measuring their dissociation time (t 1/2) over an 8-hour period. Notably, five PBK peptides (#1, #3, #6, #8, and #9) demonstrated prolonged dissociation times, exceeding 6 hours. This indicates that these peptides not only possess high binding affinity but also form stable complexes with HLA-A2 molecules, suggesting their potential as strong candidates for immunotherapeutic interventions.

The generation of peptide-specific CTLs holds significant promise for cancer immunotherapy. DCs were employed to prime naive anti-PBK CD8+ T cells within the PBMCs. Upon maturation and treatment with PBK peptides, these DCs effectively initiated the priming process by co-incubating with autologous CD8+ T cells. The subsequent assessment of antigen specificity of the peptide-induced CTLs revealed that PBK #3 and PBK #8 peptides elicited significantly higher levels of epitope-specific

CTLs compared to other peptides. Notably, the frequencies of IFN-γ producing T cells induced by PBK #3 and PBK #8 peptides were notably elevated compared to other PBK peptides, indicating robust CTL activation. The evaluation of the cytotoxic activity of the antigen-specific CTLs demonstrated their ability to effectively lyse T2 cells loaded with the corresponding PBK #3 and PBK #8 peptides. However, these CTLs showed minimal to no cytotoxicity against T2 cells loaded with irrelevant peptides, highlighting the specificity of the CTL response induced by PBK #3 and PBK #8 peptides. Overall, these findings underscore the potential of PBK #3 and PBK #8 peptides to induce antigen-specific CTL responses in vitro, suggesting their suitability for targeted immunotherapeutic strategies against PBK-expressing cancers. Further investigations into the efficacy and safety of these peptides in preclinical and clinical settings are warranted to validate their therapeutic utility.

The establishment of a mouse model to evaluate the feasibility of PBK-targeted therapies provides a crucial step towards clinical applications. The confirmation of high PBK expression in cancer cell lines, but not in normal tissues, underscores the specificity of this target, potentially reducing the risk of adverse effects.

By employing CRISPR-Cas9 gene-editing techniques to delete PBK in CT26 cells, the study reveals the impact of PBK deficiency on cancer cell behavior. The in vitro proliferation assay demonstrates that the absence of PBK does not impede the proliferative capacity of cancer cells, suggesting that PBK may not directly regulate cell growth under in vitro conditions. The analysis of MHC-I and MHC-II expression reveals no significant difference between PBK-deficient and wild-type CT26 cells, suggesting that PBK abrogation may not affect the antigenicity of cancer cells. Similarly, the expression of immune checkpoint molecules PD-L1 and PVR remains unchanged, indicating that PBK deficiency might not influence the immunogenicity.

The evaluation of tumor growth in syngeneic mouse models demonstrates a reduction in the growth of PBK-deficient CT26 tumors, highlighting the therapeutic potential of targeting PBK. Subsequent analysis of TILs reveals a significant increase in the number of CD4+ and CD8+ T cells in PBK-deficient tumors, accompanied by elevated expression of granzyme B in CD8+ T cells. These findings suggest that PBK deficiency enhances the cytotoxic potential of T cells, contributing to increased cancer cell killing within the tumor microenvironment.

Interestingly, the observed increase in T cell infiltration may be attributed to the recruitment of T cells rather than proliferation, underscoring the complex role of PBK in modulating the immune response. This differentiation is crucial for understanding the mechanism by which PBK targeting influences the immune response and could inform the development of strategies to maximize the

efficacy of such therapies. Overall, these findings highlight the potential of targeting PBK in cancer immunotherapy to augment the anti-tumor immune response and open new avenues for therapeutic interventions in cancer treatment.

REFERENCES

1. Abe, Y., et al., *Cloning and expression of a novel MAPKK-like protein kinase, lymphokine-activated killer T-cell-originated protein kinase, specifically expressed in the testis and activated lymphoid cells.* J Biol Chem, 2000. **275**(28): p. 21525-31.
2. Gaudet, S., D. Branton, and R.A. Lue, *Characterization of PDZ-binding kinase, a mitotic kinase.* Proc Natl Acad Sci U S A, 2000. **97**(10): p. 5167-72.
3. Fujibuchi, T., et al., *Expression and phosphorylation of TOPK during spermatogenesis.* Dev Growth Differ, 2005. **47**(9): p. 637-44.
4. Dougherty, J.D., et al., *PBK, a proliferating neural progenitor-specific mitogen-activated protein kinase kinase.* J Neurosci, 2005. **25**(46): p. 10773-85.
5. Brown-Clay, J.D., et al., *PBK enhances aggressive phenotype in prostate cancer via beta-catenin-TCF/LEF-mediated matrix metalloproteinases production and invasion.* Oncotarget, 2015. **6**(17): p. 15594-609.
6. Chen, J.H., et al., *Overexpression of PDZ-binding kinase confers malignant phenotype in prostate cancer via the regulation of E2F1.* Int J Biol Macromol, 2015. **81**: p. 615-23.
7. Li, S., et al., *T-LAK cell-originated protein kinase (TOPK) phosphorylation of MKP1 protein prevents solar ultraviolet light-induced inflammation through inhibition of the p38 protein signaling pathway.* J Biol Chem, 2011. **286**(34): p. 29601-9.
8. Park, J.H., et al., *Critical roles of T-LAK cell-originated protein kinase in cytokinesis.* Cancer Sci, 2010. **101**(2): p. 403-11.
9. Park, J.H., et al., *PDZ-binding kinase/T-LAK cell-originated protein kinase, a putative cancer/testis antigen with an oncogenic activity in breast cancer.* Cancer Res, 2006. **66**(18): p. 9186-95.
10. Hu, F., et al., *PBK interacts with the DBD domain of tumor suppressor p53 and modulates expression of transcriptional targets including p21.* Oncogene, 2010. **29**(40): p. 5464-74.
11. Ayllon, V. and R. O'Connor, *PBK promotes tumour cell proliferation through p38 MAPK activity and regulation of the DNA damage response.* Oncogene, 2007. **26**(24): p. 3451-61.
12. Chen, F., et al., *T-LAK cell-originated protein kinase is essential for the proliferation of hepatocellular carcinoma SMMC-7721 cells.* Cell Biochem Funct, 2013. **31**(8): p. 736-42.

13. Lei, B., et al., *PBK expression in non-small-cell lung cancer: its correlation and prognostic significance with Ki67 and p53 expression.* Histopathology, 2013. **63**(5): p. 696-703.
14. Lei, B., et al., *PBK expression correlates with mutant p53 and affects patients' prognosis and cell proliferation and viability in lung adenocarcinoma.* Hum Pathol, 2015. **46**(2): p. 217-24.
15. Zhu, F., et al., *Bidirectional signals transduced by TOPK-ERK interaction increase tumorigenesis of HCT116 colorectal cancer cells.* Gastroenterology, 2007. **133**(1): p. 219-31.
16. Siegel, R.L., et al., *Colorectal cancer statistics, 2020.* CA Cancer J Clin, 2020. **70**(3): p. 145-164.
17. Wei, S.C., C.R. Duffy, and J.P. Allison, *Fundamental Mechanisms of Immune Checkpoint Blockade Therapy.* Cancer Discov, 2018. **8**(9): p. 1069-1086.
18. Tumeh, P.C., et al., *PD-1 blockade induces responses by inhibiting adaptive immune resistance.* Nature, 2014. **515**(7528): p. 568-71.
19. Ganesh, K., et al., *Immunotherapy in colorectal cancer: rationale, challenges and potential.* Nat Rev Gastroenterol Hepatol, 2019. **16**(6): p. 361-375.
20. Yu, I.R.E., A. Dakwar, and K. Takabe, *Immunotherapy: Recent Advances and Its Future as a Neoadjuvant, Adjuvant, and Primary Treatment in Colorectal Cancer.* Cells, 2023. **12**(2).
21. Mandal, R., et al., *Genetic diversity of tumors with mismatch repair deficiency influences anti-PD-1 immunotherapy response.* Science, 2019. **364**(6439): p. 485-491.
22. Zhang, X., et al., *Neoadjuvant Immunotherapy for MSI-H/dMMR Locally Advanced Colorectal Cancer: New Strategies and Unveiled Opportunities.* Front Immunol, 2022. **13**: p. 795972.
23. Li, S.K.H. and A. Martin, *Mismatch Repair and Colon Cancer: Mechanisms and Therapies Explored.* Trends Mol Med, 2016. **22**(4): p. 274-289.
24. Le, D.T., et al., *PD-1 Blockade in Tumors with Mismatch-Repair Deficiency.* N Engl J Med, 2015. **372**(26): p. 2509-20.
25. Kaczmarek, M., et al., *Cancer Vaccine Therapeutics: Limitations and Effectiveness-A Literature Review.* Cells, 2023. **12**(17).
26. Coulie, P.G., et al., *Tumour antigens recognized by T lymphocytes: at the core of cancer immunotherapy.* Nature Reviews Cancer, 2014. **14**(2): p. 135-146.
27. Ahmed, H., et al., *Role of T cells in cancer immunotherapy: Opportunities and*

challenges. Cancer Pathog Ther, 2023. **1**(2): p. 116-126.

28. Haen, S.P., et al., *Towards new horizons: characterization, classification and implications of the tumour antigenic repertoire.* Nat Rev Clin Oncol, 2020. **17**(10): p. 595-610.
29. Mapara, M.Y. and M. Sykes, *Tolerance and cancer: mechanisms of tumor evasion and strategies for breaking tolerance.* J Clin Oncol, 2004. **22**(6): p. 1136-51.
30. Grimmett, E., et al., *Cancer vaccines: past, present and future; a review article.* Discov Oncol, 2022. **13**(1): p. 31.
31. Fan, T., et al., *Therapeutic cancer vaccines: advancements, challenges, and prospects.* Signal Transduct Target Ther, 2023. **8**(1): p. 450.
32. Wick, D.A., et al., *Surveillance of the tumor mutanome by T cells during progression from primary to recurrent ovarian cancer.* Clin Cancer Res, 2014. **20**(5): p. 1125-34.
33. Mittal, D., et al., *New insights into cancer immunoediting and its three component phases elimination, equilibrium and escape.* Current Opinion in Immunology, 2014. **27**: p. 16-25.
34. Melero, I., et al., *Therapeutic vaccines for cancer: an overview of clinical trials.* Nat Rev Clin Oncol, 2014. **11**(9): p. 509-24.
35. Buonaguro, L. and M. Tagliamonte, *Peptide-based vaccine for cancer therapies.* Front Immunol, 2023. **14**: p. 1210044.
36. Hobernik, D. and M. Bros, *DNA Vaccines-How Far From Clinical Use?* Int J Mol Sci, 2018. **19**(11).
37. Duan, L.J., et al., *Potentialities and Challenges of mRNA Vaccine in Cancer Immunotherapy.* Front Immunol, 2022. **13**: p. 923647.
38. Hollingsworth, R.E. and K. Jansen, *Turning the corner on therapeutic cancer vaccines.* NPJ Vaccines, 2019. **4**: p. 7.
39. Strum, S., et al., *State-Of-The-Art Advancements on Cancer Vaccines and Biomarkers.* Am Soc Clin Oncol Educ Book, 2024. **44**(3): p. e438592.
40. Guo, L., et al., *Colorectal Cancer Immune Infiltrates: Significance in Patient Prognosis and Immunotherapeutic Efficacy.* Front Immunol, 2020. **11**: p. 1052.
41. Newman, A.M., et al., *Robust enumeration of cell subsets from tissue expression profiles.* Nat Methods, 2015. **12**(5): p. 453-7.
42. Simpson, A.J., et al., *Cancer/testis antigens, gametogenesis and cancer.* Nat Rev Cancer, 2005. **5**(8): p. 615-25.
43. Shi, X., et al., *Decitabine enhances tumor recognition by T cells through upregulating*

the MAGE-A3 expression in esophageal carcinoma. Biomed Pharmacother, 2019. **112**: p. 108632.

44. Jurtz, V., et al., *NetMHCpan-4.0: Improved Peptide-MHC Class I Interaction Predictions Integrating Eluted Ligand and Peptide Binding Affinity Data.* J Immunol, 2017. **199**(9): p. 3360-3368.

45. Schuler, M.M., M.D. Nastke, and S. Stevanovikc, *SYFPEITHI: database for searching and T-cell epitope prediction.* Methods Mol Biol, 2007. **409**: p. 75-93.

국문 요약

항암 면역치료를 위한 PBK 타겟 항암 백신 개발에 관한 연구

PBK (PDZ-binding kinase)는 세포주기 및 유사분열을 조절하는 역할을 갖는 인산화 효소이다. PBK는 p38, ERK, MAPK 등과 관련된 여러 신호 경로의 활성화를 조절하여 세포 증식, DNA 손상 반응 및 세포 사멸 등의 여러 과정에 관여한다. 특히 빠르게 증식하는 여러 암종에서 PBK가 과발현되며, 종양 억제인자인 p53과 상호작용하고, 세포주기 조절 단백질인 p21을 감소시켜 암 발생 및 진행을 촉진한다고 알려져 있다. 이것은 PBK가 암의 발생, 발달, 전이에 결정적인 역할을 한다는 것을 나타낸다. PBK가 정상조직에서는 매우 낮은 수준으로 발현되거나 아예 존재하지 않고 생식 세포 및 암세포에서 발현되는 것이 알려져 있다. PBK가 작용하는 암 성장 촉진 메커니즘과 관련하여 PBK를 표적으로 하는 억제제 등의 연구가 활발하게 이루어지고 있지만, PBK를 항암 면역 치료법의 타겟으로 삼는 연구는 알려지지 않았다. 대장암에서 PBK 발현과 종양 면역 사이의 상관관계 및 그 예후를 분석하였다. 생물정보학 분석에 기초하여, 우리는 대장암 환자에서 PBK 발현 증가가 긍정적인 예후를 예측하며, CD8+ T 세포, CD4+ T 세포, NK 세포, M1 macrophage와 같은 항암 면역 기능을 갖는 세포들의 종양 침윤 정도가 PBK 발현과 양의 상관관계가 있다는 것을 발견하였다. PBK를 타겟하는 항암 백신을 개발하여 새로운 항암 치료제로 그 가능성을 평가하였다. 표적 특이적인 CD8+ T 세포의 항암 면역 반응을 유도할 수 있는 PBK 펩타이드 백신을 설계하고 in vitro와 in vivo에서 그 효능을 평가하였다. 새롭게 디자인된 펩타이드를 수지상세포에 표지하여 백신 특이적인 T 세포 항암 면역반응을 하였다. 선정한 백신 후보 물질과 면역 체크포인트 억제제 anti-PD-L1의 병용투여 효능을 마우스 모델을 이용하여 평가하였다. 본 연구의 결과는 PBK를 타겟하는 항암 백신이 효과적인 항암 면역 반응을 유도할 수 있는 새로운 항암 치료제로 가능성을 제시한다.